Design and Analysis of Induction Heating System with Parallel Resonance Inverter

Gokhan Yalcin*, Yasar Birbir **, Huseyin Calik***

*Department of EEE, Institute of Pure and Applied Sciences, Marmara University, Istanbul, Turkey
** Department of EEE, Faculty of Technology, Marmara University, Istanbul, Turkey
*** Department of EEE, Vocational School of Technical Sciences, Istanbul University-Cerrahpasa, Istanbul, Turkey

(gokhanyalcin04@msn.com, ybirbir@marmara.edu.tr, hcalik@istanbul.edu.tr)

‡ Corresponding Author; Gokhan Yalcin, Department of EEE, Institute of Pure and Applied Sciences, Marmara University, Istanbul, Turkey, Tel: +90 **216 777 1860**, gokhan.yalcin@marun.edu.tr

Received: 13.02.2020 Accepted:02.04.2020

Abstract- In comparison to the conventional heating systems, the induction heating systems have not only higher efficiency but also quite shorter processing time. Depending on their working conditions, they do not dissipate heat to the environment and cause pollution, and this makes them be environmentally friendly. The fact that the system does not allow any case such as explosion, combustion or injury reveals the reliability of this system. Because of the superiorities mentioned above, day by day it is more widely used in the modern industry treatments such as surface hardening, welding, tempering, rolling, heating, and melting. Whereas the induction heating systems with series resonance are designed as single-phase and low-powered in general, the induction heating systems with parallel resonance are used in high-powered and high-frequency three-phase industrial applications. In this study, an induction heating system which has 17 kW power enabling melting of brass material containing 58% copper, and has a frequency of 14,5 kHz, three-phase, voltage sourced, and full-bridged rectifier with parallel resonance inverter is designed. MATLAB simulation of the designed system is performed, and an analysis is carried out with the obtained results. In the operation of the system, a high current of 1132 A is provided on the load during the resonance. Thus, it is provided that the high value of short circuit current circulating in the brass material, which is considered as a load, produces heat in the part, and melts the metal part in a quite short time.

Keywords- Induction heating; parallel resonance inverter; simulink; metal part; melting

1. Introduction

Induction heating is a kind of contact-free heating method which is used to heat metallic work pieces at the specified temperature and time. The general principle of induction heating is based upon the transformation of electrical energy into heat energy by taking advantage of electromagnetism effect of the electrical energy [1].

Electromagnetic induction, which is the basis of induction heating, was found by Michael Faraday in 1831. According to the transformer theory, as the basic principle of it, a current flows through the primer when a voltage is applied on it. Any change in the direction and amount of the primer current causes change upon the magnetic field, and this induces a voltage over the secondary coils. When the secondary coil, on which voltage is induced, is short-circuited on its both ends, and the short circuit current will flow on it [2]. According to Lenz's Law, this current creates a flux in the opposite direction of the original flux. The flux in the opposite direction will cause Foucault current transfer, which will complete its cycle transforming into the heat in the secondary. When the secondary coil is winded as a single turn in the transformer, a very high

current will flow through it since the current is inversely proportional to the applied number of turns. When the output power of the circuit is chosen as high at the kW levels, the current on the load will increase further and therefore the heat on the load as well. Thus, it will melt the metal part accepted as the secondary coil. Furthermore, according to Lenz's Law, this flux can be directly changed with the frequency, which is created in the opposite direction to itself by the currents occurred depending upon the voltages that are induced and showing heating effect [3]. In the induction heating applications; three-phase, voltage sourced, and full-bridged parallel resonance inverters are widely in use in the industry. Besides that, there are single-phase, current sourced, series resonance inverters. Moreover, switching circuit half-bridged or E-class inverters are also in use [4]. When the system is designed as a three-phase, a power factor which is greater than the one of single-phase system is provided. As the fluctuations will be less in the rectified voltage, the size and the capacity of the filter capacitor will be reduced[5].

When a simple switching element is preferred for the inverter circuit, only the frequency control can be performed by using the switching device. At that time, to control the voltage in the rectifier section which usually consists of the thyristors, a full controlled rectifier is used. Yet, in such cases, the thyristor increases not only the cost but also the dimensions of the circuit. The fact that the frequency and voltage are controlled from two different places makes the control more complicated. When a switching element like IGBT is used in the inverter circuit, both the frequency control and the voltage control can be made by using IGBT, and the controlled rectifier will not be needed. Rectifier section which was built as a simple bridge with diodes will be enough. This will reduce the cost and size of the circuit, thus makes the control more convenient. The current at the input of the current source inverter is supplied through the serial inductance filter. In the voltage sourced inverters, the voltage supply is made with a parallel capacitor connected to the input. Voltage control via voltage sourced circuit usage is made by switching elements. In this way, it ensures having a simpler and cheap system by using an uncontrolled rectifier at the input of the circuit. This not only reduces the cost but also simplifies the control process[6].

Switching circuit of the inverter designed as full bridged provides an advantage in output power and frequency controls. Due to the high-frequency switching stresses occur on the switch, and switch voltage is always greater than the voltage source. At the same time, it has a single-switch circuit structure that limits the control of output power. The bridge-type resonance inverters have more than one switch rules out such limitation. For such investors, switch voltage is limited by the voltage source. Because of the fact that E-class resonance inverters require fewer members than bridge-type resonance inverters, they have a single switch structure just due to their low-costs. Consisting of two switching members, half-bridged resonance inverters have a lower cost than four-switch, full-bridged inverter[7]. In this study, the full-bridge inverter is designed and analyzed because of the fact that full-bridged inverters have more output power than half-bridged inverters and they have more advantage than single-switch inverters[8]- [9]. By means of parallel connection of R-L-C members in the resonance circuit, it enables load current adjustment with charge and discharge of resonance capacitors. Moreover, in the parallel resonance case, a current which is higher than that of series resonance is supplied on the load. Thus, it enables the melting of large pieces which are difficult to be melted[10].

The studies in the literature have been examined and in this study, the frequency and voltage control has been provided by the inverter circuit thanks to the use of IGBT switching device in the inverter circuit. In this way, the rectifier circuit was constituted by diodes instead of SCR. Thus, there is no need to control the rectifier circuit and the cost was reduced. This design has been made and

analyzed by taking into account the magnetic circuit parameters as well as thermal calculations, and is unique with respect to other studies in the literature. In addition, with this proposed circuit, it is ensured that the metal part is melted in a shorter time with the high power and high frequency values determined by the results of the study.

Induction heating systems significantly contribute to energy efficiency in terms of melting and reusing metals. In this study; The designed inverter structure has high usability in one-phase high power renewable energy systems. The designed inverter can be used to drive the loads desired to operate at the resonance frequency with the energy obtained from the renewable energy system.

2. Working Principle of The System

In the parallel resonance inverters, resonance elements L-C are connected parallel to each other. Fig.1 shows an induction heating system with a three-phase voltage source full bridge parallel resonant inverter[8]. As seen on the figure, the circuit consisting of three-phase diode bridge, filter capacitor, A_1, A_2, A_3, A_4 switches, chock coil, and C-L-R parallel resonance circuit. After the mains voltage is rectified by the uncontrolled rectifier, it is transferred to the filter capacitor. Filter capacitor regulates the voltage despite the fluctuations in the input voltage. It acts as a voltage source by using its ability to hold voltage on its ends, and it provides a regulated and constant voltage to the inverter. Switching the line voltage on the input of inverter, it is transformed into an alternative voltage in the desired frequency. The inverted diode is connected to each switch in order to provide current flow both in positive and negative directions. Serial chock coils regulate the current, which are connected to the input of the resonance circuit. Chock coil supplies the resonance circuit with a regulated constant current and prevents sudden current pulses to the resonance capacitor. Resonance capacitor feeds the load with regulated voltage and the heating process is performed [11]-[12].

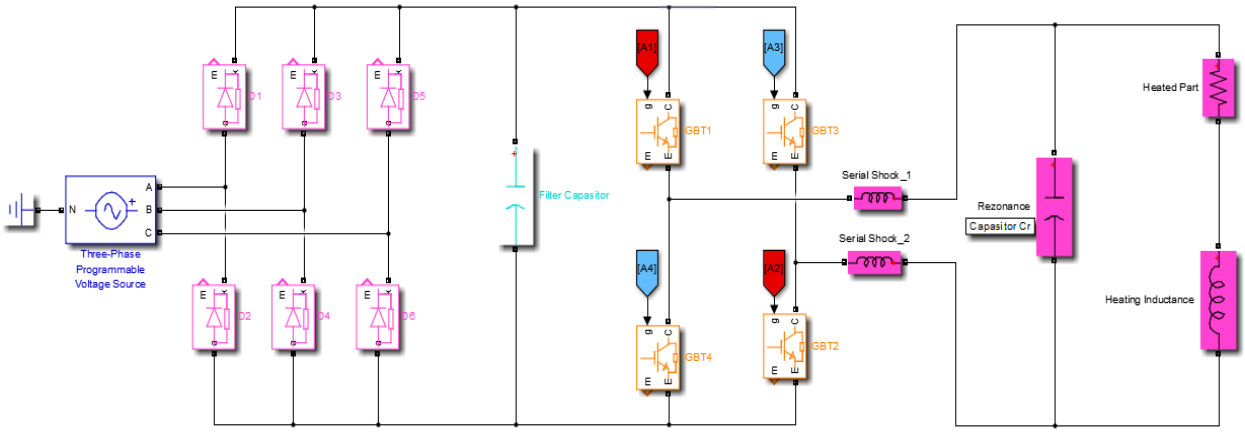

Figure 1. Voltage sourced full-bridged parallel resonance induction heating circuit.

As long as A_1, A_2, A_3, A_4 semiconductor switches are active, there is positive current flow through them. When there is a cut-off for the semiconductor switches, there is a negative current flow upon the inverted connected diodes. Switching elements are driven by the square wave voltages at the switching frequency according to the switching sequence order. In this alternating switching operation, the duty cycle rate must be less than 50%. The time, when both switches located on the one branch remain in insulation during the switching period, is called as dead time. The diodes connected in reverse parallel to the switches are designed in order to keep the power loss at minimum[13]. When A_1 switch is turn off, D_2 and D_4 diodes give the energy stored on the resonance capacitor back to the source in the dead time interval and enable A_2 and A_4 switches to be on the zero current status before taking them the

turn-on status. The same status is true for other two switches; here by reverse recovery problem is removed because zero current is provided on both sides after the diode is turn off mode. On-off losses occur only due to the high-frequency switching. In order to obtain alternative voltage on the load,A_1 and A_2switches are turn on the first half of the switching period, and A_3, A_4 switches are turn on the second half of the switching period [14].

As distinct from the serial resonance circuits, a chock coil is used in the parallel resonance circuit, except connecting the capacitor and the coil parallel to each other. The chock coil connected in series between the inverter and the capacitor, smooths the current pulses with its self-inductance characteristics which charge the capacitor at the converter output. It also prevents the fluctuations and protects circuit elements by snubbing possible rapid changes on the load current[15]. Likewise, in the event that there is a short circuit on the load side, it also softens the next current pulse. This prevents overheating of the transformer and reduces the probability of burning of the diodes in the inverter[16].

During the operation of resonance circuit, chock coil filters the current received from the inverter circuit at the end of a period. Therefore, a phase difference occurs between the current and the voltage[17]. In this way, the current will be lagged the voltage. In the time of current filter of chock coil, the voltage leads, and resonance capacitor will charge as the peak value of the voltage. By the way, the current to be received from the chock coil and the heating coil, and therefore the heated metal part will be fed too. In the following period, the load will be supplied through the capacitor in the section, in which chock coil filters the current. In this way, the chock coil not only regulates the current but also creates a system which provides the continuous feeding of the load [18].

3. Analysis of the System

In this study, the step of the system design, the input phase voltage is 380 V, and network frequency is 50 Hz. First of all, in the system output, output power is chosen as 17 kW, and frequency is chosen as 14,5 kHz. As output voltage, it is taken as 250 V, and MATLAB simulation is performed following the calculations of parameters. The topology of the circuit is created on the system, and the parameters of devices are determined according to the topology and output values. MATLAB simulation is performed by using these values; thus, graphics are obtained. After the graphics are interpreted, the positives and negatives of parallel resonance operations are analysed.

As to switching member, an IGBT is chosen whose power loss is low in a value close to BJT and whose switching speed is high in a value close to MOSFET. The current value of IGBT used in the design is calculated as seen in Eq.(1). Considering the tolerances, an IGBT with a current rating of 200 A was selected.

$$I_{DC} = \frac{P}{V} = \frac{17.10^3}{210} = 80{,}95 \text{ A} \quad (1)$$

DC bus voltage of the system is about 380 V, and inverter AC output voltage is 380 V. In the event that the IGBTs on the inverter circuit are chosen as the 80,95 A nominal value is obtained at the Eq.(2).

$$R_l = \frac{V_C}{I_C} = \frac{380}{80{,}95} = 4{,}69\ \Omega \quad (2)$$

Because it is τ = 3,33 ms in the three-phase rectifier, the capacitance value of the filter capacitor can be obtained as seen in the Eq.(3), and voltage value can be obtained as seen in the Eq.(4).

$$C = \frac{5\tau}{R_l} = \frac{5 \cdot 3{,}33}{4{,}69} = 3550\ \mu\text{F} \quad (3)$$

$$V_D = 380 \cdot 1{,}342 = 510\ \text{V} \quad (4)$$

The diode current used in the rectifier is calculated as seen in the Eq.(5).

Considering the tolerances, it is evaluated to use a bridge diode with a current rating of 100 A.

$$I_D = \frac{80,95}{3} = 27 \text{ A} \quad (5)$$

In order to limit the instantaneous high currents occurring in the resonance circuit, a shock coil specific to this circuit has been designed. The choke is divided into equal values on two separate arms. Thus, It is provided that the targeted current passes over the part to be heated. In the work, the more stable load current is passed compared to conventional induction heating systems.

In the system, in the resonance circuit, two pieces serial shock coils are connected between the inverter and resonance capacitor. The current of the coil, whose inductance value is chosen as 150 µH, is calculated as seen in the Eq.(6).

$$I_{RM} = \frac{P}{U} = \frac{17 \cdot 10^3}{250} = 68 \text{ A} \quad (6)$$

It is designed considering that the inductance of resonance circuit and represented heating coil wire diameter is 10 mm and wall thickness is 1,25 mm.

3.1 Calculation of the Resonance Circuit

In the resonance circuit, calculations were performed upon coil, capacitor, and heated part. Performed calculations are investigated under two sections as thermal calculations and magnetic circuit calculations.

In thermal calculations, the amount of heat needed to melt the part, and the melting time were calculated. In addition to these, in the magnetic circuit calculations, some values are calculated such as immersion depth, resistance, and reactance

$Q = m.\ c.\ \Delta_t = 6,04.94.(800\text{-}25) = 440 \text{ kcal} = 1842,19 \text{ kJ}$ (9)

Time required for melting of the part in the system, which has output power as 17 kW, is calculated in the Eq.(10).

$$t = \frac{Q}{P} = \frac{1842,19.10^3}{17.10^3} = 108 \text{ s} \quad (10)$$

Assuming that 17 KW power is transferred to the system for melting without system loss, the melting process takes place in 108 seconds.

values, impedance, coil efficiency, power coefficient, apparent power, flow current and applied voltage for the metal part and the heating coil.

3.2 Thermal Calculations

Because the heating coil is designed as the helical in the system, it is considered that the heated member is a brass part having the copper in the rate of 58% in it, and in the shape of a cylinder. The volume of the part, which is designed as 90 mm in height, and 100 mm in diameter, is calculated in the Eq.(7), and its mass is calculated in the Eq.(8) where *V*: Volume of the part to be heated (m3), *h*: Height of the part to be heated (m), *m*: Mass of the part to be heated (kg), *d*: Density of the part to be heated (kg/m3).

$$V = \pi . r^2 . h = \pi . (0,5)^2 . 0,9 = 706,858.10^{-3} \text{ dm}^3 \quad (7)$$

(7)

$$M = d.V = 8,55.706,858.10^{-3} = 6,04 \text{ kg} \quad (8)$$

When the brass part is considered to start melting at 800ºC, the heat energy to be created upon the brass part which has 6,04 kg mass, and whose temperature will be increased from 25 ºC to 800ºC during the operation is calculated in Eq.(9) where *Q*: Heat energy to be obtained by the part to be heated (cal), *c*: Specific heat of the part to be heated (cal/kg.ºC), Δ*t*: Temperature change of the part to be heated (ºC), *P*: Electrical power required for melting of part (W).

3.3. Magnetic Circuit Calculations

Considering that the brass material selected a metal part, is heated up to the 800 ºC in order to be melted, the resistivity at 800ºC and average self-resistivity of the metal part can be calculated during the heating process can be calculated as seen in the Eq.(11),(12).The parameters of the system are shown in the Table 1.

$\rho_{w800}=\rho_{w25}.(1+\alpha.\Delta t)$

$=5{,}9.10^{-8}.[1+0{,}002.(800-25)]=15{,}04.10^{-8}\Omega$ (11)

$$\sqrt{P_m}=\frac{1}{2}\left(\sqrt{P_{25}}+\sqrt{P_{800}}\right)$$

$$=\frac{1}{2}\left(\sqrt{5{,}9.10^{-8}}+\sqrt{15{,}04.10^{-8}}\right)=3{,}15.10^{-4}$$

$P_m = 9{,}92.10^{-8}\ \Omega$ (12)

The immersion depth of the metal part can be calculated as seen in the Eq.(13).

$$\delta=\sqrt{\frac{2P_m}{\mu.w}}=\sqrt{\frac{2.9{,}944.10^{-8}}{50.4.\pi.10^{-7}.2.\pi.14{,}5.10^{3}}}=0{,}18.10^{-3}\text{mm} \quad (13)$$

where, δ: Immersion Depth (mm),P_m: Average resistivity of material (Ωm), μ_0: Magnetic permeability of air, μ_r: Relative magnetic permeability of material, ω:Angular frequency (R/s).

p and q values used in the resistance calculation of the heated metal part can be calculated as in the Eq.(14). These p and q values do not depend upon only to the geometrical structure but also frequency, self-resistivity, and magnetic permeability[19].

$$p=\frac{2}{1{,}23+\frac{d_w}{\delta}}=\frac{2}{1{,}23+\frac{100.10^{-3}}{0{,}18.10^{-3}}}=0{,}00359$$

$$q=\frac{2}{\frac{d_w}{\delta}}=\frac{2}{\frac{100.10^{-3}}{0{,}18.10^{-3}}}=0{,}00360 \quad (14)$$

K value of the metal part can be calculated as seen in Eq.(15).

$$K=\frac{2.\pi.f.\mu_0.N_c^{\,2}}{l_c}$$

$$=\frac{2.\pi.14{,}5.10^{3}4.\pi.10^{-7}.3^2}{110.10^{-3}}=9{,}36 \quad (15)$$

The resistance value of the heated brass material during the resonance moment can be calculated as seen in the Eq.(16).

$R_W = K.(\mu_r.p.A_w)$

$= 9{,}36.(50.0{,}00359.7{,}853.10^{-3}) =13{,}2\ \text{m}\Omega$ (16)

Table 1. Design target specifications of the single ended resonant inverter

Three Phase Unity Power Factor Converter					
Inverter Parameters		**Working Piece Parameters**		**Coil Parameters**	
Output Power	17 KW	Cylindrical load diameter	d_w= 100 mm	Coil diameter	d_c =130 mm
DC Input Voltage	510 V	Working piece length	l_w = 90 mm	Coil length	l_c=110 mm
Resonant Frequancy	14,5 KHz	Relativy permeability of brass part	μ_r = 50	Resistivity of cooper	ρ_{25} =0,017 μΩm
Power Factor of the coil	0,45 (lagging)	Resistivity of brass part	ρ_{25} =0,059 μΩm	Temperature coefficient of resistivity	α_{25}= 0,004 K^{-1}
		Temperature coefficient of resistivity	α_{25} = 0,002 K^{-1}	Number of turns	N_c=3
		Permeability of free space	$\mu_0 = 4\pi.10^{-7}$		

Average self-resistivity of the heating coil can be calculated as seen in Eq.(17), and the immersion depth can be calculated as in the immersion depth of the heated metal part in Eq.(18).

$\rho_{c800}=\rho_{c25}.(1+\alpha.\Delta t)$

$=17.10^{-9}.[1+0{,}004.(800-25)] = 69{,}7.10^{-9}\ \Omega\text{m}$ (17)

$$\delta_c=\sqrt{\frac{2P_c}{\mu.w}}=\sqrt{\frac{2.69{,}7.10^{-9}}{1{,}26.10^{-6}.2.\pi.14{,}5.10^{3}}}=1{,}1.10^{-3}\text{mm} \quad (18)$$

where; N_c: Applied number of heating coil, l_c: Length of heating coil (mm), d_w: Diameter of heated metal part (m), R_w: Resistance of heated metal part (Ω), A_w: Section of heated metal part (m^2), P_c: Average resistivity of heating coil (mΩ), δ_c: Immersion depth of heating coil (mm), p: Flow value, q: Flow value.

There is a very close similarity between the induction heating system and transformer, the

heating coil is designed by calculating the resistance and reactance values on the equivalent circuit in Fig.2.

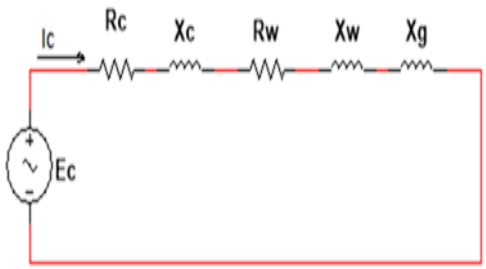

Figure 2. The electrical equivalent circuit of induction heating coil

where; R_c: Resistance of heating coil (Ω), X_w: Reactance of heated metal part (Ω), X_c: Reactance of heating coil (Ω), X_g: Reactance of Air gap (Ω), coil resistance R_c can be calculated as seen in Eq.(19) depending upon physical parameters of the coil.

$$R_c = K.\left(\frac{k_r.\pi.d_c.\delta_c}{2}\right) = 9{,}36.\left(\frac{1{,}5.\pi.130.10^{-3}.1{,}1.10^{-3}}{2}\right) = 3{,}15\ \text{m}\Omega \quad (19)$$

d_c: Coil diameter (mm), k_r: Coil coefficient which is determined on the coil, the space between the coil conductors is taken into account. Coil reactance and coil resistance is approximately taken as per Eq.(20).

$$x_c = R_c = 3{,}15\text{m}\Omega \quad (20)$$

Air gap reactance value X_g is considered as serial to the coil and metal part. Which is calculated in Eq.(21).

$$x_g = K.\ A_g = 9{,}36.\ 1{,}649.10^{-3} = 15{,}43\text{m}\Omega \quad (21)$$

The reactance of the metal part is calculated by putting q instead of p in the resistance formula of the metal part in Eq.(22).

$$x_w = K\ (\mu_r.q.A_w) = 9{,}36\ (50.\ 0{,}0036.7{,}85.10^{-3}) = 13{,}22\ \text{m}\Omega \quad (22)$$

The ratio of the resistance of the metal part to the total resistance gives the efficiency of the coil. According to this, the efficiency of the coil can be obtained as seen in Eq.(23).

$$\eta = \frac{R_w}{R_c+R_w} = \frac{13{,}2}{3.15+13{,}2} = 0{,}80 \quad (23)$$

Equivalent impedance of the circuit is calculated as seen in Eq.(24).

$$Z = \sqrt{(R_w + R_c)^2 + \left(x_w + x_c + x_g\right)^2}$$

$$Z = \sqrt{(13{,}2 + 3{,}15)^2 + (13{,}22 + 3{,}15 + 15{,}43)^2} = 35{,}75\ \text{m}\Omega \quad (24)$$

Power coefficient *Cos φ* of the circuit is found by the ratio of total resistance to the impedance in Eq.(25).

$$\text{Cos}\ \phi = \frac{R_{total}}{z} = \frac{R_w+R_c}{Z} = \frac{13{,}2 + 3{,}15}{35{,}75} = 0{,}46 \quad (25)$$

Because the power coefficient is obtained from the ratio of active power to the apparent power at the same time, the apparent power can be calculated as seen in Eq.(26).

$$S = \frac{P}{\eta.cos\ \varphi} = \frac{17.10^3}{0{,}80.0{,}46} = 46{,}195\ \text{KVA} \quad (26)$$

Ampere-turn (*Ic.Nc*) and applied voltage (*Ec/Nc*) are more important parameters in the coil design. These parameters can be calculated as seen in Eq. (27),(28).

$$I_c.N_c = \sqrt{\frac{S}{\frac{Z}{{N_c}^2}}} = \sqrt{\frac{46{,}195.10^3}{\frac{35{,}75.10^{-3}}{9}}} = 3410\ \text{ampere-turn} \quad (27)$$

Where, I_c: Effective value of current in the coil, N_c: Coil number of turn, E_c: Effective voltage of coil.

$$\frac{E_c}{N_c} = \sqrt{S.\frac{Z}{{N_c}^2}} = \sqrt{\frac{46{,}195.10^3.\ 35{,}75.10^{-3}}{9}} = 13{,}54\text{Volt/turn} \quad (28)$$

I_c current in the coil is obtained by dividing the total ampere-turn into the number of coil turn in Eq.(29).

$$I_c = \frac{I_c.N_c}{N_c} = \frac{3410}{3} = 1136\ \text{A} \quad (29)$$

AC voltage occurred in the coil is obtained by dividing the applied voltage of coil into the number of coil turn in Eq.(30).

$$E_c = N_c \frac{E_c}{N_c} = 13{,}54 \ .3 = 40{,}63 \text{ V} \quad (30)$$

The voltage on the material is calculated in the Eq.(31), considering that there is a transformer conversion rate of 1:3 between the material and the heating coil.

$$E_w = \frac{40{,}63}{3} = 13{,}54 \text{ V} \quad (31)$$

Calculated *Rw, Rc, Xw, Xc, Xg* values of resonance circuit devices and total inductance value in the induction heater can be determined in Eq. (32),(33) [20].

$$X_{TOTAL} = X_w + X_c + X_g = (13{,}22 + 3{,}15 + 15{,}43).\ 10^{-3}$$
$$= 31.8 \text{ m}\Omega \quad (32)$$

$$L_{r_L} = \frac{X_{TOTAL}}{\omega} = \frac{31{,}8.10^{-3}}{2.\pi.14{,}5.10^3} = 0{,}35 \ \mu\text{H} \quad (33)$$

In the event it is considered that the inductive reactance and capacitive reactance values are equal to each other in the resonance instant, capacitance value can also be calculated in Eq.(34).

$$x_{L_{TOTAL}} = x_{C_{rL}}$$

$$C_{rL} = \frac{1}{(2\pi f_r)^2 . L_{rL}} = \frac{1}{(2.\pi.14{,}5.10^3)^2 . 0{,}35.10^{-6}}$$
$$= 344{,}22 \ \mu\text{F} \quad (34)$$

The resonance capacitor may overheat due to changes in the load current. For this reason, the melting performance of the system decreases. The user can solve this problem by letting the capacitor cool down. This is done by placing cooler aluminum rods between the PCB boards that make up the capacitor. Thanks to this application, the melting is prevented from taking longer than the targeted time.

4. System Simulation and Results

Values of members are calculated in the study and MATLAB simulation is created. The circuit seen in Fig.3 is used in the simulation.

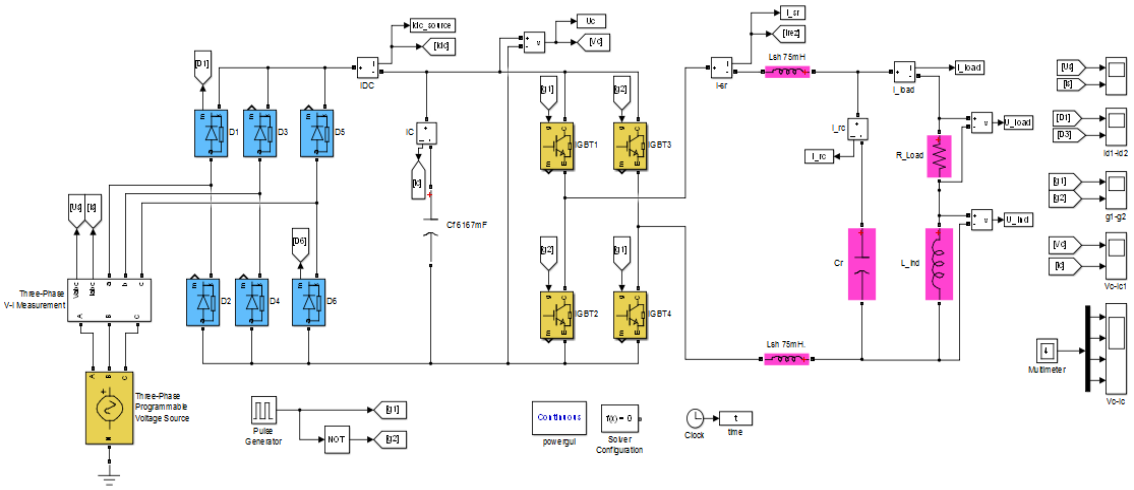

Figure 3. Simulation Circuit of Operation

The calculated values for the simulation on the circuit, for which the topology is determined, are given to the members on the circuit. 2 pieces of signal detectors are connected to send the signal to their gates in order to turn on the IGBTs, and the square wave signal is applied. To perform measurements, voltmeters and ammeters, and scopes are connected to each of their ends in order to provide the graphics.

In Figure 4, it is seen that the resonance capacitor voltage reached up to 248 V peak value. Moreover, the frequency value is calculated as 14,5 kHz from the period value of the curve. Because of the negative-directed high voltage, which is received in

the capacitor during the first operation, more peak values are seen in the negative directions in the capacitor voltage diagram.

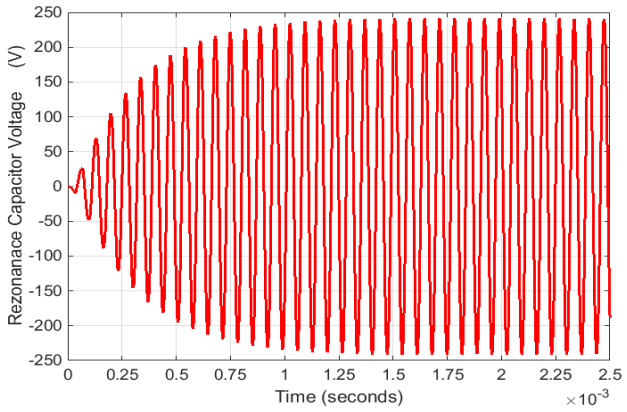

Figure 4. Resonance capacitor voltage

In Figure 5, it is seen on the graphic that there are approximately 243 V voltages on the heating coil. In Fig.6, there are 15 V voltages on the heated part, mentioned with ohmic voltage drop. It is understood that the 244 V voltages are shared by the coil and heated part. It is seen that voltages of capacitor, heating coil and heated part come into existence in the same direction. Because the heated part member is in ohmic characters, it is seen that there is scarcely any peak on its graphic.

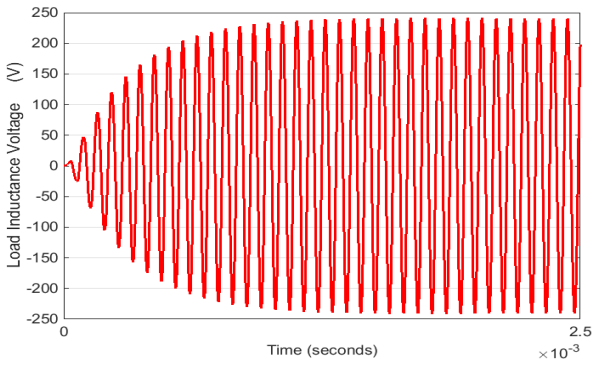

Figure 5. Heating coil voltage

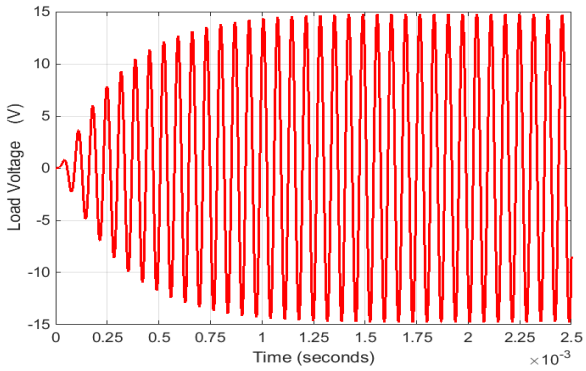

Figure 6. Heated part voltage

In Figure 7, when graphics of the current passing through the chock coil at the resonance circuit input is investigated, it is seen that approximately 1132A current passes through on both of directions. By means of current storage ability of the coil, it is seen that it takes the current on it for each current pulse, the current reaches the peak value, and it transmits the current on it to the resonance circuit.

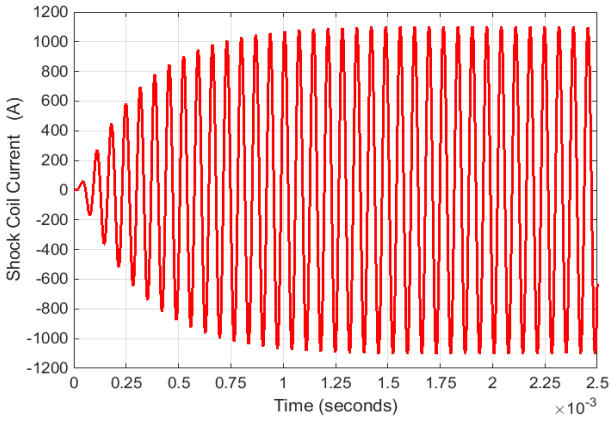

Figure 7. Shock coil current

Figure 8 is investigated, it is seen that the capacitor, Load, and inverter output currents. It is seen that positive and negative directed currents balance each other after a while, and they reach in the level of 1134A current. It is seen that these peak

values nearly the chock coil current 1132 A.

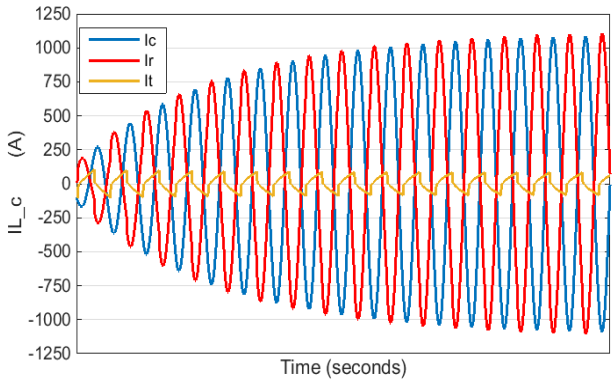

Figure 8. Heated metal part and Resonance capacitor current

In Figure 9, when the current graphic of the heated part is investigated, it is seen that the current continuously changes with switching and charge-discharge status of the resonance capacitor and it creates a sine graphic. The 1132A current value read on the current graphic of the metal part is the current value, when the part reached the highest heat at the resonance time. The load current and resonance capacitor currents are about 180 degrees phase shift. Therefore, the inverter output current is nearly resistive and 80 A.

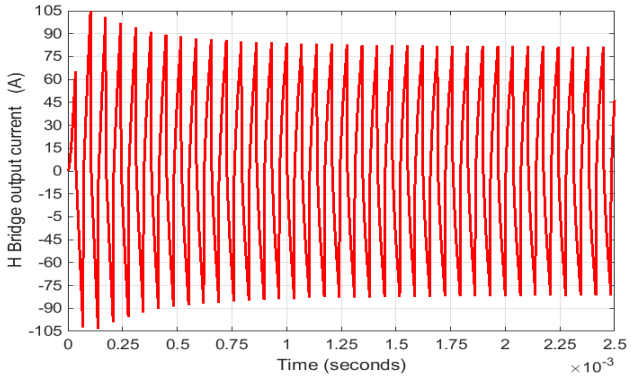

Figure 9. H Bridge output current

When the voltage value, which is measured from the load ends, is proportioned to the part resistance, load current is calculated as seen in Eq.(35).

$$I_L = \frac{U_L}{R} = \frac{15}{13{,}2.10^{-3}} = 1136\ \text{A} \qquad (35)$$

The value read on the current graphic of heated part, load current value calculated by using arm-currents method, current value calculated by ampere-turn method, current value passing through heating coil, and value of load current calculated with Ohm`s law are determined separately, and it is determined that they are nearly equal to each other. As calculated in five diverse ways, it is seen that there is an approximately 1132 A load current during the resonance instant. Moreover, 15 V voltages are measured on the load. In this situation, in the system, on which output power is designed as 17 kW, it is seen that melting operation is performed by consuming a 16.98 kW power as seen in the Eq.(36) when the losses are taken into account on the inverter circuit.

$$P_L = U_L.I_L = 15.1132 = 16{,}98\ \text{kW} \qquad (36)$$

(36)

Input power of the system is calculated by multiplying the linear voltage, which is applied upon the parallel resonance inverter, with direct current as seen in Eq.(37).

$$P_g = U_d.I_d = 530.\ 39{,}77 = 21{,}078\ \text{kW} \qquad (37)$$

The efficiency of the system is calculated as seen in the Eq.(38) by taking the ratio of output power to the input power applied on the system, which is obtained from the metal part while the induction heating system is operating in parallel resonance.

$$\eta_{system} = \frac{16{,}98\ 10^3}{21{,}078.10^3} = 0{,}80 \qquad (38)$$

With the review of the studies in the literature, the system can be shown as an innovation in terms of providing a high current transition of 1132 A under a very small voltage of 15V on the load.

During the parallel resonance operation, it is seen that there are microscopic stress and current at a very high level on the load. Moreover, at all graphics that belong to the resonance circuit, 14,5 kHz value is taken as resonance frequency. Therefore, the induction furnaces having parallel resonance inverters are mostly used to melt hard metals, and three-phase industrial furnaces, such as scrap furnaces, etc. are used for the applications requiring high power and high-frequency.

In the proposed system, the thermal and magnetic calculations made were verified by simulation results. The targeted results were obtained in both methods. The results are in accordance with each other.

5. Conclusion

In this study, an induction heating system with 17kW output power of the parallel resonance inverter was designed to melt brass material containing 58% copper. The used inverter which has a frequency of 14.5kHz, is a voltage sourced and in the full bridge structure. Power Electronics and Drives MATLAB simulation of the designed system is performed, and an analysis is carried out based on the obtained results. In the system, after the three-phase input voltage is rectified with uncontrolled rectifier, it is regulated with the filter capacitor. This direct voltage is transformed into an alternating voltage with full-bridged inverter in the requested high-frequency. With the 200A, 300V IGBT switch on the inverter, the system and its members are resonated. So, an 1132 A high-current flow is provided upon the load. Under high frequency, the heat generated by the high current causes the metal part to melt in about 108 seconds. The results obtained by the analytical method were also confirmed by simulation. A coil in series with the input of the current source inverter is placed. This coil provides a constant current to the inverter. By this means, the inverter is made more robust to any short-circuit. However, since there is no constant voltage at the inverter input, the voltage control is provided by the controlled rectifier which is used at the inverter input. The switching elements in the inverter circuit can only perform the frequency control. In this study, it was preferred to use a voltage source inverter. Since a constant voltage is obtained at the inverter input, both the voltage and frequency control are provided by the inverter. Therefore, a three-phase full wave and uncontrolled rectifier is used at the inverter input. The use of uncontrolled rectifiers has reduced the size of the circuit and the cost. It simplified the control of the system as well. Thus, it has been found out that parallel resonance inverters with voltage source provide an efficient operation at high output power. The filter capacitor and resonance capacitor in the system can be consisted of a single capacitor or formed with capacitor groups. Both capacitors should be cooled. This cooling can be achieved by aluminum rods to be placed between the capacitor banks. The heating coil design is tubular with an internal diameter of approximately 12 mm and a thickness of 1 mm. In this study, it was seen that the analytical modelling of the parallel resonance induction heating system, and dynamic modelling based on simulink were fully consistent. It is provided to determine the dynamic stresses on the system components before the hardware installation of the parallel resonance induction heating system at a given power. The designed system is recommended as a system with short process time, efficient, safe, and easy temperature control.

References

[1]S. Kubota, " The Optimal Composition of Diesel Particulate Filter Using Induction Heating", IEEE 18th International Power Electronics and Motion Control Conference (PEMC), 2018.

[2]S.S. Choi, C.W. Lee, I.D. Kim and J.H. Jung, "New Induction Heating Power Supply for Forging Applications Using IGBT Current-Source PWM Rectifier and Inverter", 21st International Conference on Electrical Machines and Systems (ICEMS), 2018.

[3]A. Naval, H. Sarnago, I. Lope and O. Lucia, "Improved Litz wire manufacture process using resonant power converter-based induction heating", The international journal for computation and mathematics in electrical and electronic engineering, Vol. 36, No. 2, 2017.

[4]N. Domingo, L.A. Barragan, J.M.M. Montiel, A. Dominguez, "Fast power–frequency function estimation for induction heating appliances", Electronics Letters, Vol. 53, No. 7, 2017.

[5]R. Molay, S. Mainak, "A commutation strategy for IGBT-based CSI-fed parallel resonant circuit for induction heating application", Sadhana-Academy Proceedings In Engineering Sciences, Volume 42, Issue 2, 2017.

[6]I. Colak, O. Kaplan, "Design and Implementation of Sensorless DC Voltage Regulation for Shunt Active Power Filter Based Single Phase P-Q Theory", 8th IEEE International Conference on Renewable Energy Research and Applications(ICRERA), Brasov, Romania, 2019.

[7]K. Kajiwara, T. Kazuki, S. Ikeda, N. Matsui, F. Kurokawa, "Performance Mechanism of Active Clamp Resonant SEPIC Converter in Renewable Energy Systems", 8th IEEE International Conference on Renewable Energy Research and Applications(ICRERA), Brasov, Romania, 2019.

[8]S.I. Annie, K.M. Salim, Z. Tasneem, "Frequency Analysis of a ZVS Parallel Quasi Resonant Inverter for a Solar Based Induction Heating System", International Conference on Electrical Computer and Communication Engineering (ECCE), 2017.

[9]A. Attab, H. Zeroug, B. Meziane, "A dual constant power control for metal induction heating system using series resonant inverters", 11th IEEE International Conference on Compatibility, Power Electronics and Power Engineering (CPE-POWERENG), 2017.

[10]H. Lill, A. Allik, M. Hovi, K. Loite, A. Annuk, "Integrated Smart Heating System in Historic Buildings", 7th IEEE International Conference on Smart Grid(icSmartGrid), 2019.

[11]K.S. Zachariah, M. Vennila, "High Power Frequency Parallel Resonance Inverter With Bridgeless Rectifier For Induction Heating Application", International Conference on Electrical Electronics and Optimization Techniques (ICEEOT) IEEE, 2016.

[12]H. Benbouhenni, Z. Boudjema, A. Belaidi, "Direct Power Control of a DFIG Fed by a Seven Level Inverter Using SVM Strategy", International Journal of Smart Grid – ijSmartGrid, Vol. 3, No. 2, 2019.

[13]H. Sarnago, O. Lucia, "Dual-output boost resonant full bridge topology and its modulation strategies for high-performance induction heating applications", IEEE Transactions on Industrial Electronics, Vol. 63, No. 6, 2016.

[14]A. Belkaid, I. Colak, K. Kayisli, R. Bayindir, "Design and Implementation of a Cuk Converter Controlled by a Direct Duty Cycle INC-MPPT in PV Battery System", International Journal of Smart Grid – ijSmartGrid, Vol. 3, No. 1, 2019.

[15]J. Zgraja, "Susceptibility of the LLC resonance Generator for Induction Heating on Changes in Load Parameters Caused by Heating the Charge", 978-1-5386-8255-5/18 IEEE, Lodz, Poland, 2018.

[16]H. Zhang, A. Wu, "Bridge-arm current reduction in DC-AC inverter", International Journal of Electronics, Taylor & Francis, Vol. 105, No. 10, 2018.

[17]S.V. Madhavi, G.T. Ram Das, "Linear and Non-Linear Carrier Control of Soft Switched Isolated Boost Converter for Low Voltage Fuel Cell Applications", International Journal of Renewable Energy Research-IJRER, Vol. 9, No. 2, 2019.

[18]O. Lucia, P. Maussion, E.J. Dede, J.M. Burdio, "Induction Heating Technology and Its Applications: Past Developments, Current Technology, and Future Challenges" ,IEEE Transactions on Industrial Electronics Year, Volume 61, Issue 5 ,2014.

[19]B.S. Sazak, "A New Unity Power Factor Quasi-Resonant Induction Heater", Department of

Electronics and Information Technology, University of Glamorgan, Wales, 1997.

[20]V.C. Valchev, T.P. Todorova, "Design Considerations of Inductors for Induction Heating of Fluids", Proc. XXV International Scientific Conference Electronics-ET2016, September 12 - 14, 2016.